A L-MMSE DS-CDMA Detector for MIMO/BLAST Systems with Frequency Selective Fading

João Carlos Silva[1], Nuno Souto[1], António Rodrigues[1],Américo Correia[2], Francisco Cercas[2], Rui Dinis[3]
[1] Instituto Superior Técnico/IT, Torre Norte 11-11, Av. Rovisco Pais 1, 1049-001 Lisboa, Portugal, joao.carlos.silva@lx.it.pt, nuno.souto@lx.it.pt, antonio.rodrigues@lx.it.pt
[2] ADETTI/IT, Torre Norte 11-08, Av. Rovisco Pais 1, 1049-001 Lisboa, Portugal, americo.correia@lx.it.pt, francisco.cercas@lx.it.pt
[3] CAPS-IST, CAPS, Av. Rovisco Pais 1, 1049-001 Lisboa, Portugal, rdinis@ist.utl.pt

***Abstract*—The L-MMSE (Linear Minimum Mean Square Error) DS-CDMA (Direct Sequence-Code Division Multiple Access) receiver algorithm was adapted for the MIMO/BLAST (Multiple Input, Multiple Output / Bell Laboratories Layered Space Time) system in order to increase capacity, considering frequency selective fading (multipath). The receiver achieves perfect decoding in the absence of noise and reasonable values of cross-correlation between the users' signature sequences, independent of modulation or loading (excluding overloading). This is crucial for cases of a fully loaded system, in which all antennas are transmitting different messages using all of the available spreading codes. To assess the system performance, we considered the uncoded UMTS HSDPA (High Speed Downlink Packet Access) standard.**

Keywords- MMSE, MIMO, BLAST, multipath, HSPDA, UMTS

I. Introduction

Digital communication using MIMO, sometimes called a "volume-to volume" wireless link, has recently emerged as one of the most significant technical breakthroughs in modern communications. Just a few years after its invention the technology is already part of the standards for wireless local area networks (WLAN), third-generation (3G) networks and beyond.

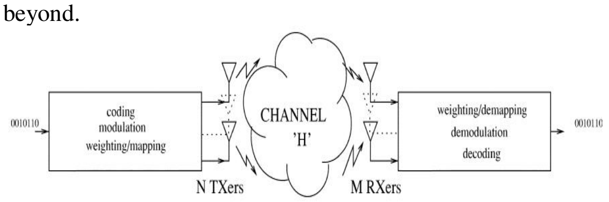

Figure 1 : MIMO scheme

MIMO schemes are used in order to push the capacity and throughput limits as high as possible without an increase in spectrum bandwidth, although there is an obvious increase in complexity. For N TX and M RX antennas, we have the capacity equation [1], [2], [3]

$$C_{EP} = \log_2\left(\det\left(\mathrm{I}_M + \frac{\rho}{N} HH'\right)\right) \text{ b/s/Hz}$$

where H is the channel matrix, H' is the transpose-conjugate of H and ρ is the SNR at any RX antenna. Foschini [1] and Telatar [4] both demonstrated that the capacity grows linearly with m=min(M,N), for uncorrelated channels.

Therefore, it is possible to augment the capacity/throughput by any factor, depending on the number of TX and RX antennas. The downside to this is the receiver complexity, sensitivity to interference and correlation between antennas, which is more significant as the antennas are closer together. For a 3G system, for instance, it is inadequate to consider more than 2 or 4 antennas at the UE (User Equipment)/ mobile receiver.

Note that, unlike in CDMA where user's signatures are quasi-orthogonal by design, the separability of the MIMO channel relies on the presence of rich multipath which is needed to make the channel spatially selective. Therefore, MIMO can be said to effectively *exploit* multipath.

The receiver for such a scheme is obviously complex; due to the number of antennas, users and multipath components, the performance of a simple RAKE/ MF (Matched Filter) receiver (or enhanced schemes based on the MF) always introduces a significant amount of noise, that doesn't allow for the system to perform at full capacity. Thus being, the MMSE receiver was built for such cases, acting as an equalizer. Other related works only considered a similar receiver for MIMO flat fading [5] (with gains very dependent on channel correlation) and the case of SISO (Single Input, Single Output) with multipath [6], (although the latter had some imprecision in the analytical treatment of the scheme).

The structure of the paper is as follows. In Section II, the MMSE receiver for MIMO with multipath is introduced. The simulation setup is detailed in Section III and Section IV comments on the obtained results. The main conclusions are drawn in Section V.

II. MMSE Receiver

A standard model for a DS-CDMA system with K users (assuming 1 user per physical channel) and L propagation paths is considered. The symbols (QPSK/16QAM) are spread by a Walsh-Hadamard code with length equal to the Spreading Factor (*SF)*.

Assuming that the transmitted signal on a given antenna is of the form

$$\boldsymbol{e}(t)_{tx=1} = \sum_{n=1}^{N}\sum_{k=1}^{K} \boldsymbol{A}_{k,tx}\boldsymbol{b}_{k,tx}^{(n)}\boldsymbol{s}_k(t-nT),$$

where N is the number of received symbols, $\boldsymbol{A}_{k,tx} = \sqrt{E_k}$, E_k is the energy per symbol, $\boldsymbol{b}_{k,tx}^{(n)}$ is the n-th

This work has been partially funded by the B-Bone project (IST-2003-507607), and by a grant of the Portuguese Science and Technology Foundation (FCT).

transmitted data symbol of user k and transmit antenna tx, $\boldsymbol{s}_k(t)$ is the k-th user's signature signal (equal for all antennas) and T denotes the symbol interval.

The received signals of a MIMO system with N_{TX} transmit and N_{RX} receive antennas, on one of the receiver's antennas can be expressed as:

$$\boldsymbol{r}_{v_{rx=1}}(t) = \sum_{tx=1}^{N_{TX}} \boldsymbol{e}_{tx}(t) * \boldsymbol{c}_{tx,rx}(t) + \boldsymbol{n}(t)$$

where $\boldsymbol{n}(t)$ is a complex zero-mean AWGN (Additive White Gaussian Noise) with variance σ^2, $\boldsymbol{c}_{tx,rx}(t) = \sum_{l=1}^{L} \boldsymbol{c}_{tx,rx,l}^{(n)} \delta(t-\tau_l)$ is the impulse response of the radio link between the antenna tx and rx (assumed equal for all users using this link), $\boldsymbol{c}_{tx,rx,l}$ is the complex attenuation factor of the l-th path of the link, τ_l is the propagation delay (assumed equal for all antennas) and * denotes convolution. The received signal on can also be expressed as:

$$\boldsymbol{r}_{v_{rx=1}}(t) = \sum_{n=1}^{N} \sum_{tx=1}^{N_{TX}} \sum_{k=1}^{K} \sum_{l=1}^{L} \boldsymbol{A}_{k,tx} \boldsymbol{b}_{k,tx}^{(n)} \boldsymbol{c}_{tx,rx}(t) \boldsymbol{s}_k(t - nT - \tau_l) + \boldsymbol{n}(t)$$

Using matrix algebra, the received signal can be represented as $\boldsymbol{r}_v = \boldsymbol{SCAb} + \boldsymbol{n}$, where $\boldsymbol{S}$, $\boldsymbol{C}$ and $\boldsymbol{A}$ are the spreading, channel and amplitude matrices respectively.

The spreading matrix $\boldsymbol{S}$ has dimensions $(SF \cdot N \cdot N_{RX} + \psi_{MAX} \cdot N_{RX}) \times (K \cdot L \cdot N \cdot N_{RX})$ ($\psi_{\max}$ is the maximum delay of the channel's impulse response, normalized to number of chips, $\psi_{MAX} = \left\lceil \frac{\tau_{\max}}{T_c} \right\rceil$ where T_c is the chip period), and is composed of sub-matrices $\boldsymbol{S}_{RX}$ in its diagonal for each receive antenna $\boldsymbol{S} = \mathrm{diag}(\boldsymbol{S}_{\mathrm{RX},1}, \ldots, \boldsymbol{S}_{\mathrm{RX},\mathrm{N}_{\mathrm{RX}}})$. Each of these sub-matrices has dimensions $(SF \cdot N + \psi_{MAX}) \times (K \cdot L \cdot N)$, and are further composed by smaller matrices $\boldsymbol{S}_n^L$, one for each bit position, with size $(SF + \psi_{MAX}) \times (K \cdot L)$. The $\boldsymbol{S}_{RX}$ matrix structure is made of $\boldsymbol{S}_{\mathrm{RX}} = [\boldsymbol{S}_{\varepsilon,1}, \ldots, \boldsymbol{S}_{\varepsilon,\mathrm{N}}]$, with

$$\boldsymbol{S}_{\varepsilon,\mathrm{n}} = \begin{bmatrix} 0_{(\mathrm{SF}\cdot(n-1))\times(\mathrm{K}\cdot\mathrm{L})} \\ \boldsymbol{S}_{\mathrm{n}}^{\mathrm{L}} \\ 0_{(\mathrm{SF}\cdot(\mathrm{N}-\mathrm{n}))\times(\mathrm{K}\cdot\mathrm{L})} \end{bmatrix}.$$

The $\boldsymbol{S}^L$ matrices are made of $K \cdot L$ columns; $\boldsymbol{S}_n^L = \left[\boldsymbol{s}_{\mathrm{col}(k=1,l=1),n}, \ldots, \boldsymbol{s}_{\mathrm{col}(k=1,l=L),n}, \ldots, \boldsymbol{s}_{\mathrm{col}(k=K,l=L),n} \right]$. Each of these columns is composed of $\boldsymbol{s}_{\mathrm{col}(kl),n} = \left[0_{(1\times\mathrm{delay}(l))}, \varphi_n(k)_{1\times SF}, 0_{(1\times(\psi_{MAX}-\mathrm{delay}(l)))} \right]^T$, where $\boldsymbol{\varphi}_n(k)$ is the combined spreading & scrambling for the bit n of user k.

These $\boldsymbol{S}^L$ matrices are either all alike if no long scrambling code is used, or different if the scrambling sequence is longer than the SF. The $\boldsymbol{S}^L$ matrices represent the combined spreading and scrambling sequences, conjugated with the channel delays. The shifted spreading vectors for the multipath components are all equal to the original sequence of the specific user.

$$\boldsymbol{S}_n^L = \begin{bmatrix} \boldsymbol{S}_{1,1,1,n} & & \cdots & \cdots & \boldsymbol{S}_{K,1,1,n} & & \\ \vdots & \ddots & \boldsymbol{S}_{1,1,L,n} & \cdots & \vdots & \ddots & \boldsymbol{S}_{K,1,L,n} \\ \boldsymbol{S}_{1,SF,1,n} & & \vdots & \cdots & \boldsymbol{S}_{K,SF,1,n} & & \vdots \\ & \ddots & \boldsymbol{S}_{1,SF,L,n} & \cdots & \cdots & \ddots & \boldsymbol{S}_{K,SF,L,n} \end{bmatrix}$$

Note that, in order to correctly model the multipath interference between symbols, there is an overlap between the $\boldsymbol{S}^L$ matrices, of ψ_{MAX}. As opposed to the SISO multipath case presented in [6], there is no matrix clipping for the last multipath components.

The channel matrix $\boldsymbol{C}$ is a $(K \cdot L \cdot N \cdot N_{RX}) \times (K \cdot N_{TX} \cdot N)$ matrix, and is composed of N_{RX} sub-matrices, each one for a receive antenna $\boldsymbol{C} = \begin{bmatrix} \boldsymbol{C}_{RX,1} \\ \vdots \\ \boldsymbol{C}_{\mathrm{RX},\mathrm{N}_{RX}} \end{bmatrix}$. Each $\boldsymbol{C}_{RX}$ matrix is composed of N $\boldsymbol{C}^{KT}$ matrices alongside its diagonals.

$$\boldsymbol{C}_{\mathrm{RX},\mathrm{N}_{RX}} = \begin{bmatrix} \boldsymbol{C}_{1,N_{RX}}^{KT} & & \\ & \ddots & \\ & & \boldsymbol{C}_{N,N_{RX}}^{KT} \end{bmatrix}$$

Each $\boldsymbol{C}^{KT}$ matrix is $(K \cdot L) \times (K \cdot N_{TX})$, and represents the fading coefficients for the current symbol of each path, user, transmit antenna and receive antenna. The matrix structure is made up of further smaller matrices alongside the diagonal of $\boldsymbol{C}^{KT}$, $\boldsymbol{C}^{KT} = \mathrm{diag}\left(\boldsymbol{C}_{K=1}^{T}, \ldots, \boldsymbol{C}_{K=K}^{T}\right)$, with $\boldsymbol{C}^{T}$ of dimensions $L \times N_{TX}$, representing the fading coefficients for the user's multipath and tx-th antenna component.

$$\boldsymbol{C}^{KT} = \begin{bmatrix} c_{1,1,1} & \cdots & c_{N_{TX},1,1} & & & \\ \vdots & & \vdots & & & \\ c_{1,L,1} & \cdots & c_{N_{TX},L,1} & & & \\ & & & \ddots & & \\ & & & c_{1,1,K} & \cdots & c_{N_{TX},1,K} \\ & & & \vdots & & \vdots \\ & & & c_{1,L,K} & \cdots & c_{N_{TX},L,K} \end{bmatrix}$$

The A matrix is a diagonal matrix of dimension $(K \cdot N_{TX} \cdot N)$, and represents the amplitude of each user per transmission antenna and symbol, $\mathrm{A} = \mathrm{diag}\left(\mathrm{A}_{1,1,1}, \ldots, \mathrm{A}_{\mathrm{N}_{\mathrm{TX}},1,1}, \ldots, \mathrm{A}_{\mathrm{N}_{\mathrm{TX}},\mathrm{K},1}, \ldots, \mathrm{A}_{\mathrm{N}_{\mathrm{TX}},\mathrm{K},\mathrm{N}}\right)$.

Vector b represents the information symbols. It has length $(K \cdot N_{TX} \cdot N)$, and has the following structure $\mathrm{b} = \left[\mathrm{b}_{1,1,1}, \ldots, \mathrm{b}_{\mathrm{N}_{\mathrm{TX}},1,1}, \ldots, \mathrm{b}_{1,\mathrm{K},1}, \ldots, \mathrm{b}_{\mathrm{N}_{\mathrm{TX}},\mathrm{K},1}, \ldots, \mathrm{b}_{\mathrm{N}_{\mathrm{TX}},\mathrm{K},\mathrm{N}} \right]^T$. Note that the bits of each TX antenna are grouped together in the first level, and the bits of other interferers in the second level. This is to guarantee that the resulting matrix to be inverted has all its non-zeros values as close to the diagonal as possible. Also note that there is usually a higher correlation between bits from different antennas using the same spreading code, than between bits with different spreading codes.

Finally, the n vector is a $(N \cdot SF \cdot N_{RX} + N_{RX} \cdot \psi_{MAX})$ vector with noise components to be added to the received vector r_v, which is partitioned by N_{RX} antennas, $\boldsymbol{r}_v = \left[\boldsymbol{r}_{1,1,1}, \ldots, \boldsymbol{r}_{1,SF,1}, \ldots, \boldsymbol{r}_{N,1,1}, \ldots, \boldsymbol{r}_{N,SF+\psi_{MAX},1}, \ldots, \boldsymbol{r}_{N,1,N_{RX}}, \ldots, \boldsymbol{r}_{N,SF+\psi_{MAX},N_{RX}}\right]^T$.

The MMSE algorithm yields the symbol estimates, y_{MMSE}, which should be compared to vector *b*,

$$y_{MF} = (SCA)^H r_v \quad , \quad y_{MMSE} = (E_M)^{-1} y_{MF}$$
$$R = A \cdot C^H \cdot S^H \cdot S \cdot C \cdot A \quad E_M = R + \sigma^2 I$$

where σ^2 is the noise variance of *n*, y_{MF} is the matched filter output and E_M is the Equalization Matrix (cross-correlation matrix of the users' signature sequences after matched filtering, at the receiver).

The expected main problem associated with such scheme is the size of the matrices, which assume huge proportions. Due to the multipath causing Inter-Symbolic Interference (ISI), the whole information block has to be simulated, requiring the use of a significant amount of memory and some computing power for the algebraic operations, with emphasis on the inversion of the E_M in the MMSE algorithm.

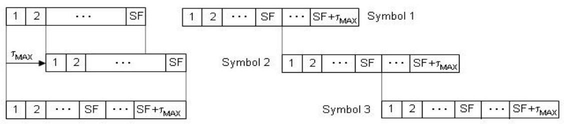

Figure 2 : Symbol overlap due to multipath, causing ISI

However, if the sparseness of the matrices is taken into account, only a fraction of the memory and computing power is required. As it was previously illustrated, all matrices are sparse and consist of sub-matrices that are sparse themselves.

The most troublesome matrix to deal with is the E_M, due to its inversion. The E_M has all its elements concentrated on the main diagonal, reaching high levels of sparseness. For instance, in a maximum-loading simulation case using 16QAM modulation, 1024 bits (N=256 symbols) per channel and antenna, L=2 multipaths (the second multipath with a 1 chip delay, resembling the IndoorA or PedestrianA channel) and MIMO order of Mo=2 (Mo TX and Mo RX antennas), the sparseness was around $1 - \frac{(nz=784384)}{((K=16)\cdot(TX=2)\cdot(N=256)=8192)^2} \approx 99\%$, where *nz* is the number of non-zero elements (Figure 3, left).

For the considered cases, that already took into account a large delay spread, we can see that the Matrix's Diagonal Width (MDW) is $(KL \cdot TX) \cdot \frac{3}{2} = 96$, which divided by the Matrix's Width (MW) of 8192 equals roughly MDW=1.2%MW. The complexity of the matrix inversion can be lowered from the traditional $o\left(MW^3\right)$ complexity to an upper bound $o\left(MW \cdot MDW^2\right)$, by using normal Gauss-Jordan elimination. Another aspect of the E_M is that it is Hermitian positive definite, and thus can be decomposed using the Cholesky decomposition. Since it is a banded matrix (with all elements concentrated on its diagonal), there is no Cholesky fill-in since the band is dense (cases with small chip delays (Figure 3, right)), and thus presents itself as if the Sparse Reverse Cuthill-McKee ordering algorithm [7] had been applied to it. Also, optimized banded solver algorithms can be employed, taking further advantage of the matrix's characteristics, reducing memory and complexity by an additional factor of 2. When scrambling is not used, and a very slow channel is simulated, the E_M can be represented solely by its first $K \cdot TX$ lines, and simpler inversion algorithms discussed in [12] for a similar case in SISO TD-CDMA, can be applied.

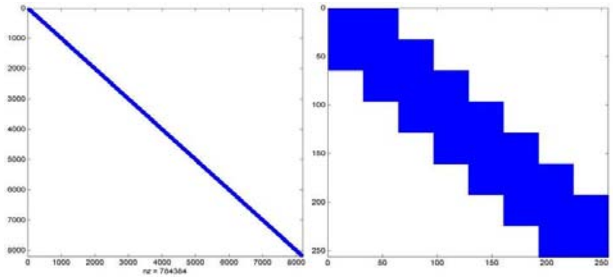

Figure 3 : (left) – *EM* for 2 tap case, K=16, TX=2 (right) – diagonal close-up for same case

Many commercially available algorithms are suited for this; for this work the simulation tool, Matlab, took this into account, when performing the matrix inverse, via the use of LAPACK [8], a multi-author FORTRAN subroutine library widely known by the mathematics community.

Two problems for the E_M are that it might become ill-conditioned when the system is fully loaded [9] (depending on the cross-correlations between the users' signature sequences), and that it might loose its positive definite property due to round-offs. In order to overcome these problems, the E_M was rounded at $1e^{-14}$.

III. SIMULATION SETUP

This work was inspired on the uncoded 3G HSDPA standard, and thus considers a SF=16 using Hadamard codes, QPSK and 16QAM modulation, a chip rate of 3.84 Mcps and a Gold-sequence scrambling code. Each TX antenna can thus host a maximum of 16 channels, with a user per channel. Simulations were run for MIMO orders of 1 (SISO), 2 and 4, so that all the expected future UE types were covered. Minimum (1 user per TX) and full loading (16 users per TX) was considered.

The main UMTS channels, namely Indoor A, Pedestrian A and Vehicular A (taken from [10]) were simulated. Since only 1 sample per chip was used in the simulations, the channels were adjusted to the chip delay time of 260ns, using the constant mean delay spread method [11]. For the particular case of Vehicular A, since the method yields 8 taps, with the last ones having low power levels, an adjustment was made so that only the main taps were considered. The resulting channels are depicted in Figure 4. The considered velocities were 50km/h for Vehicular A and 3km/h for the remaining channels.

IndA	delay (chips)	0	1		
	% received power	90,63%	9,37%		
PedA	delay (chips)	0	1		
	% received power	94,98%	5,02%		
VehA	delay (chips)	0	1	3	4
	% received power	49,50%	39,32%	6,23%	4,95%

Figure 4 : Resulting UMTS channels

The MMSE processor was placed immediately after the MIMO receiver. The channel and noise estimators, considered perfect, were placed alongside the receiver. After the MMSE decoding, the symbols were demultiplexed and demodulated, at which point a bit decision was made, and compared to the original message (Figure 5).

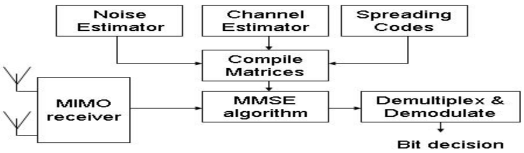

Figure 5 : MIMO scheme

The Monte Carlo method was employed for the simulations. All results were portrayed for received E_b/N_0 values *vs* BER (Bit Error Rate). In order to have a basis of comparison and a better understanding of the MMSE algorithm, the MF receiver (which is basically the unequalized MMSE) was also evaluated.

IV. SIMULATION RESULTS

A. MF Results

The MF results are important for the MMSE receiver, since it is a crucial part of the algorithm. It can be seen that, for the minimum loading case (Figure 6), results of Vehicular A are best and of Pedestrian A are worse, due to multipath diversity. The diagonal of matrix R was used for normalization of y_{MF}, instead of using just the estimated channel coefficients as is usually done for standard Rake receivers. The extra information from the EM allows minimizing the correlation effect, and thus the multipath diversity can be exploited for higher order modulations, when there is little interference, contrary to the normal Rake.

Due to interference from other antennas, and the fact that the simple MF algorithm doesn't perform any type of interference canceling nor equalization, the lowest MIMO orders provide the best results.

For the fully loaded case (Figure 7), results for Pedestrian A are better than the Vehicular A channel, due to the high amount of multipath interference. The lowest MIMO orders still provide the best results, due to the reduced interference.

B. MMSE Results

As expected, the best results were obtained for the minimum loading cases (Figures 8 and 9) of the highest MIMO orders (highest diversity), with QPSK modulation.

Since the Vehicular A channel has the greater number of taps, best results are obtained for this channel (note that perfect channel estimation is assumed). Indoor A is the second-best, since it has a second tap of greater power than the pedestrian A channel, which is predominantly a 1 tap channel.

For the fully loaded system (Figures 10 and 11), it can be seen that the situation is quite different, with the lowest MIMO orders yielding the best results, due to the reduction of interference. Thus being, for both modulations, the best and worst channel's performance are still Vehicular A and Pedestrian A, for high values of E_b/N_0. For the 16QAM case with low values of E_b/N_0, the channel's performance order is modified, with the worst being Vehicular A. This is due to the nature of the 16QAM modulation, which is dependent on the symbol's amplitude, being highly influenced by high levels of multipath interference. Note also that the performance of both Pedestrian A and Indoor A are much closer for the 16QAM case, due to the modulation's inaptness to exploit multipath when compared to the QPSK modulation.

The MMSE results are much better than for the MF alone, due to the equalization. The only performance curves from both receivers that are closer to each other are for the case of 0 interferers and SISO, where interference is minimal.

V. CONCLUSIONS

The main L-MMSE equations for frequency-selective channels and a MIMO setting were derived. For the first time, results using such a scheme were simulated and drawn for the main UMTS MIMO channels in a BLAST (in the sense of Horizontally Layered Space Time) configuration, with the HSDPA standard in mind. Both QPSK and 16QAM modulations were simulated, for both MF and MMSE without channel coding, so that the performance results using these receivers were unbiased (results for coding can be extrapolated from the uncoded BER results).

The minimum and maximum loading cases were simulated for 3 different MIMO orders, in order to cover all of the major types of services the UMTS will offer in the near future, and the different UE type terminals expected for the next few years.

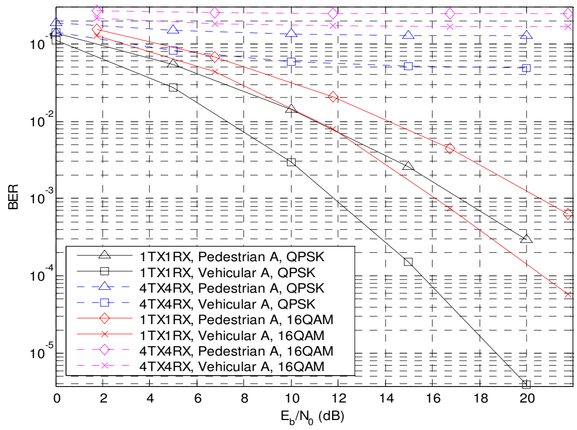

Figure 6 : MF, 0 interferers

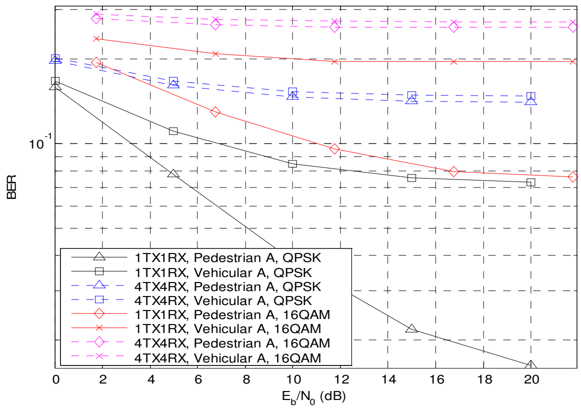

Figure 7 : MF, 15 interferers

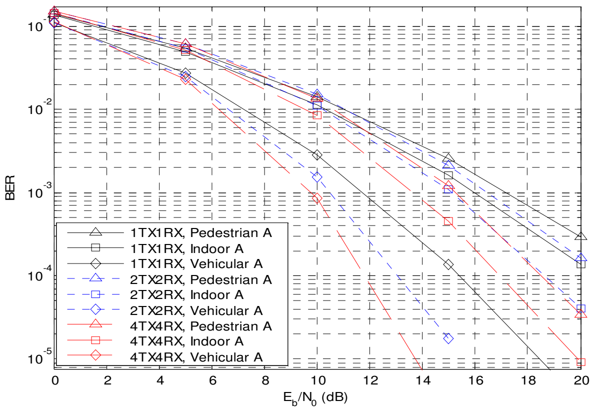

Figure 8 : MMSE, QPSK, 0 interferers

REFERENCES

[1] G. J. Foschini and M. J. Gans, "On limits of wireless communications in a fading environment when using multiple antennas," Wireless Pers. Commun., vol. 6, pp. 311–335, Mar. 1998.

[2] E. Telatar, "Capacity of multiantenna Gaussian channels," AT&T Bell Laboratories, Tech. Memo., June 1995.

[3] I. E. Telatar, "Capacity of multiantenna Gaussian channels," *Eur. Trans. Commun.*, vol. 10, no. 6, pp. 585–595, 1999.

[4] E. Telatar, "Capacity of multiantenna Gaussian channels," AT&T Bell Laboratories, Tech. Memo., June 1995.

[5] J. Shen, A. G. Burr, "Iterative Multi-User-Antenna Detector for MIMO CDMA Employing Space-Time Turbo Codes", IEEE Global Telecommunications Conference, Taipei, Taiwan, Nov. 17-21, 2002 (GLOBECOM 2002)

[6] M. Latva-aho, M. Juntti, "LMMSE Detection for DS-CDMA Systems in Fading Channels", IEEE Transactions on Communications, vol.48, no2, February 2000.

[7] George, Alan and Joseph Liu, Computer Solution of Large Sparse Positive Definite Systems, Prentice-Hall, 1981.

[8] Anderson, E., Z. Bai, C. Bischof, S. Blackford, J. Demmel, J. Dongarra, J. Du Croz, A. Greenbaum, S. Hammarling, A. McKenney, and D. Sorensen, LAPACK User's Guide (http://www.netlib.org/lapack/lug/lapack_lug.html), Third Edition, SIAM, Philadelphia, 1999.

[9] H. C. Huang, "Combined Multipath Processing, Array Processing and Multiuser Detection for DS-CDMA Channels", Ph.D dissertation, Princeton Univ., Princeton, NJ, Jan 1996.

[10] 3GPP, Deployment aspects, 3GPP TR 25.943 v5.1.0, Sophia Antipolis, France, 2002.

[11] J. C. Silva, N. Souto, A. Rodrigues, F. Cercas and A. Correia, "Conversion of reference tapped delay line channel models to discrete time channel models" , VTC03 Fall, Orlando, Florida, 6-9 Oct. 2003.

[12] M. Vollmer, M. Haardt, J. Gotze, "Comparative Study of Joint-Detection Techniques for TD-CDMA Based Mobile Radio Systems", IEEE Sel. Areas Comm., vol.19, no.8, August 2001.

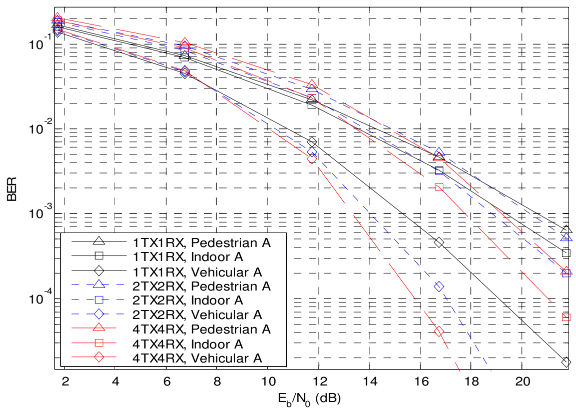

Figure 9 : MMSE, 16QAM, 0 interferers

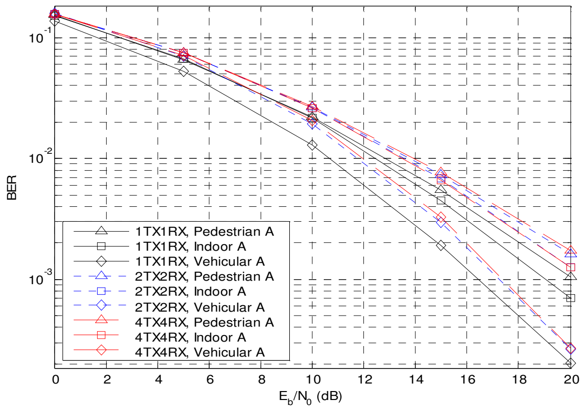

Figure 10 : MMSE, QPSK, 15 interferers

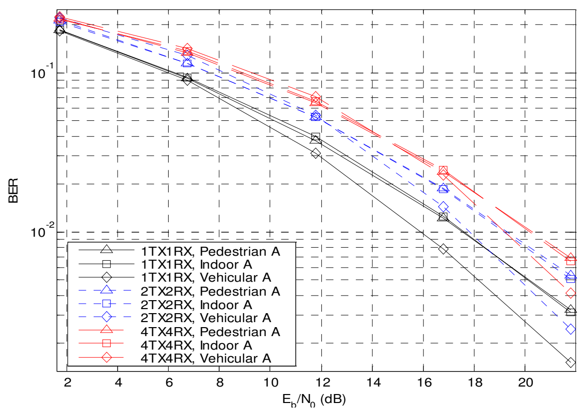

Figure 11 : MMSE, 16QAM, 15 interferers